



(This is a sample cover image for this issue. The actual cover is not yet available at this time.)

**This article appeared in a journal published by Elsevier. The attached copy is furnished to the author for internal non-commercial research and education use, including for instruction at the authors institution and sharing with colleagues.**

**Other uses, including reproduction and distribution, or selling or licensing copies, or posting to personal, institutional or third party websites are prohibited.**

**In most cases authors are permitted to post their version of the article (e.g. in Word or Tex form) to their personal website or institutional repository. Authors requiring further information regarding Elsevier's archiving and manuscript policies are encouraged to visit:**

**<http://www.elsevier.com/copyright>**



Contents lists available at SciVerse ScienceDirect

# Deep-Sea Research I

journal homepage: [www.elsevier.com/locate/dsrI](http://www.elsevier.com/locate/dsrI)



## Biogenic silica cycling during summer phytoplankton blooms in the North Pacific subtropical gyre

Jeffrey W. Krause<sup>a,\*</sup>, Mark A. Brzezinski<sup>a,b</sup>, Tracy A. Villareal<sup>c</sup>, Cara Wilson<sup>d</sup>

<sup>a</sup> Marine Science Institute, University of California, Santa Barbara, CA, USA

<sup>b</sup> Department of Ecology Evolution and Marine Biology, University of California, Santa Barbara, CA, USA

<sup>c</sup> Marine Science Institute and the Department of Marine Science, The University of Texas, Austin, Port Aransas, TX, USA

<sup>d</sup> NOAA/NMFS/SWFSC Environmental Research Division, Pacific Grove, CA, USA

### ARTICLE INFO

#### Article history:

Received 11 May 2012

Received in revised form

4 September 2012

Accepted 12 September 2012

Available online 19 September 2012

#### Keywords:

North Pacific subtropical gyre

Blooms

Diatoms

Silica production

Net silica production

Export

### ABSTRACT

Biogenic silica (bSiO<sub>2</sub>) cycling, diatom abundance and floristics were examined within summer-period diatom blooms in the North Pacific Subtropical Gyre (NPSG) in 2008 and 2009. *Hemiaulus hauckii* was the most abundant diatom observed in an expansive (100,000 km<sup>2</sup>) bloom near the subtropical front in the northeastern NPSG in 2008 and the small pennate diatom *Mastogloia woodiana* dominated a smaller (30,000 km<sup>2</sup>) bloom sampled in 2009 in the gyre interior. In both blooms, the bSiO<sub>2</sub> stock and production rates were up to an order of magnitude higher relative to non-bloom areas. Remnants of a bSiO<sub>2</sub> export event was sampled in the *H. hauckii* bloom area where the export rate at 300 m exceeded that at 150 m, and was among the highest values recorded in the NPSG. The *M. woodiana* bloom was very active with specific bSiO<sub>2</sub> production rates of 0.50–0.75 d<sup>−1</sup> and net bSiO<sub>2</sub> production rates were among the highest observed in any subtropical-gyre diatom bloom to date. Net silica production rates in the euphotic zone were strongly positive within blooms and near zero outside of blooms, consistent with an important role for blooms in bSiO<sub>2</sub> export. The difference in the areal extent of the *H. hauckii* and *M. woodiana* blooms was consistent with remote-sensing observations that blooms in the northeastern portion of the NPSG, near the subtropical front, are typically more extensive than those in the gyre interior near Hawaii Ocean Time-series station ALOHA. Initial estimates suggest that blooms in the northeast region produced 3–25 times more bSiO<sub>2</sub> in 2008 and 2009, respectively, than did blooms in the gyre interior; and due to the large areal extent these blooms, their area-integrated production of bSiO<sub>2</sub> is similar to intense diatom blooms coastal upwelling systems (e.g. Monterey Bay, Santa Barbara Channel) despite significantly lower production rates and standing stock.

© 2012 Elsevier Ltd. All rights reserved.

### 1. Introduction

Compared to blooms in other subtropical gyres, phytoplankton blooms in the North Pacific subtropical gyre (NPSG) are different in their timing and in the hydrographic conditions under which they occur. Winter convective mixing in the NPSG is weak and regular spring blooms do not ensue; instead, phytoplankton blooms occur during summer when the upper-water column stratification is at its annual maximum and macronutrient concentrations are at their annual minimum (Wilson, 2003; Dore et al., 2008; Wilson et al., 2008). This situation sharply contrasts with that in the North Atlantic Subtropical Gyre (NASG) where strong winter convection typically erodes the pycnocline and entrains nutrients into the euphotic zone, thereby stimulating a regular spring bloom after water-column restratification (Sverdrup, 1953). Summer blooms in

the NPSG interior show enhanced abundance of diazotrophs (e.g. *Trichodesmium*) and diatoms (Dore et al., 2008; Fong et al., 2008; Villareal et al., 2011, 2012); however, *Trichodesmium* is rarely observed in the northeastern NPSG near the subtropical front (Venrick, 1997; Dore et al., 2008) where satellite ocean color observations reveal blooms that are generally more expansive and that longer-lived than those in the gyre interior near the Hawaii Ocean Time-series (HOT) station ALOHA (Wilson, 2003; Wilson et al., 2008). At least some of the blooms occurring in the northeastern gyre are dominated by diatoms (Brzezinski et al., 1998; Villareal et al., 2011).

Why diatom blooms in the NPSG occur during the highly oligotrophic conditions of summer remains enigmatic. Some blooms contain diatom-diazotrophic associations (DDAs, e.g. the diatom genera *Hemiaulus* or *Rhizosolenia* and the nitrogen-fixing symbiont, *Richelia*; Villareal et al., 2011), suggesting that the biological input of fixed N may play a role in bloom initiation and development. Recently, it was also suggested that summer blooms in the northeastern NPSG can occur in response to

\* Corresponding author. Tel.: +1 805 893 7061; fax: +1 805 893 8062.  
E-mail address: [jeffrey.krause@lifesci.ucsb.edu](mailto:jeffrey.krause@lifesci.ucsb.edu) (J.W. Krause).

increased vertical mixing due to internal wave breakdown at the 30°N “critical latitude” (Wilson, 2011). A diatom bloom also requires adequate silicic acid; relative to the nanomolar levels of inorganic N and P in the surface waters of the NSPG, the silicic acid requirement is easily met as surface-water concentrations are typically 0.5–1.5  $\mu\text{M}$ . There is also evidence that the diatom taxa which dominate summer blooms have very efficient Si uptake kinetics, such that ambient silicic acid concentrations of  $\sim 1 \mu\text{M}$  would support high growth rates (Brzezinski et al., 1998; Krause et al., 2012).

While there currently is no consensus on the factor(s) initiating summer diatom blooms in the NSPG, there is clear evidence as to their importance in annual biogeochemical budgets. This is somewhat counter intuitive as diatom biomass during non-bloom periods at station ALOHA, as measured by biogenic silica ( $\text{bSiO}_2$ ) concentration, is the lowest thus far observed in the global ocean (Brzezinski et al., 2011). However, at the HOT station ALOHA the contribution of diatoms to new production exceeds both their contribution to autotrophic biomass and their estimated contribution to primary production (Brzezinski et al., 2011), implying a disproportionately important role for diatoms in carbon export. This is especially true for summer blooms which have been estimated to account for 18% of annual new production at station ALOHA (Dore et al., 2008) and recent estimates suggest that summer blooms account for 29% of the annual production of  $\text{bSiO}_2$  at ALOHA (Brzezinski et al., 2011). Blooms in the northeastern gyre near the subtropical front are typically longer-lived than those at or near ALOHA (Wilson et al., 2008), but their role in annual biogeochemical budgets is less clear. There is also evidence for a significant role for diatoms in the export of carbon to the ocean interior at ALOHA where observations from both shallow (150 m) and deep ( $\geq 2800$  m) sediment traps show an annual summer maximum in carbon export associated with increased diatom and  $\text{bSiO}_2$  export (Scharek et al., 1999a, 1999b; Karl et al., 2012). To further evaluate the contribution of summer diatom blooms to silica production and organic matter cycling in the NSPG, we examined rates of gross and net silica production, diatom abundance and taxonomic composition within summer phytoplankton blooms in the NSPG.

## 2. Methods

### 2.1. Study area and sampling

The Pacific Open-Ocean Bloom (PB) cruises were conducted aboard the R/V *Kilo Moana* from 4–19 July 2008 (PB08) and from 29 July–12 August 2009 (PB09). Using daily composite images from the Moderate Resolution Imaging Spectroradiometer (MODIS, <http://modis.gsfc.nasa.gov>), bloom regions were identified as areas with chlorophyll *a* (Chl *a*) concentrations  $\geq 0.12 \mu\text{g L}^{-1}$ . As the feature sampled in 2008 was relatively weak, visualizing the full extent of the bloom area required the [Chl *a*] threshold value to be slightly lower than the  $0.15 \mu\text{g L}^{-1}$  value used previously (Wilson et al., 2008); for consistency we use the same [Chl *a*] threshold for both PB cruises. Three regions with bloom-level [Chl *a*] were sampled, one in 2008 and two in 2009. Within each bloom region, stations were classified as representing a diatom bloom condition by meeting two criteria: (1) the  $> 10 \mu\text{m}$  size-fraction [Chl *a*] was  $> 30\%$  of the total [Chl *a*] collected on a  $> 0.4 \mu\text{m}$  filter. This threshold value represents a three-fold increase in  $> 10 \mu\text{m}$  [Chl *a*] fraction over that present under non-bloom conditions in the gyre during summer (Villareal et al., 2011), and (2) diatom numerical abundance exceeded 1000 cells  $\text{L}^{-1}$ , consistent with threshold bloom abundances previously applied in this region (e.g. Brzezinski et al., 1998; Villareal et al., 2011).

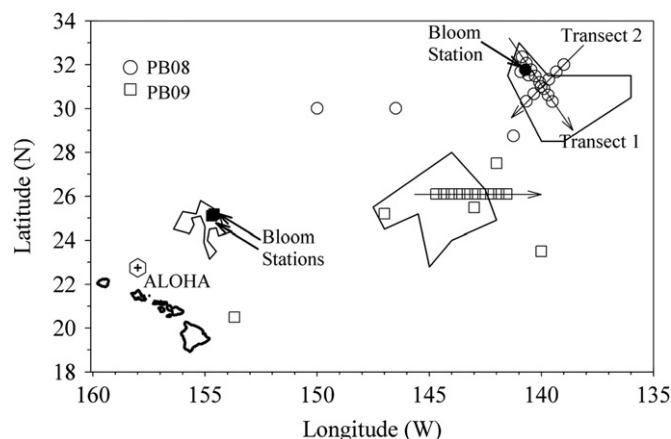


**Fig. 1.** Station locations during the PB08 and PB09 cruises, station ALOHA (HOT program) is shown for reference. Symbols are distinguished by year (PB08, circles; PB09, squares) and bloom stations (filled symbols). Outlined regions are the maximum areal extent of the MODIS-defined bloom regions ( $> 0.12 \mu\text{g L}^{-1}$  [Chl *a*]). Transect direction is denoted by arrows.

During PB08, a single bloom feature was sampled near the subtropical front northeast of Hawaii (Fig. 1). The bloom was intensifying as the ship left port in Hawaii and satellite chlorophyll levels were above the  $0.12 \mu\text{g L}^{-1}$  bloom threshold when the ship arrived at the bloom, but while the area was being sampled the satellite-observed chlorophyll levels fell below the bloom threshold. As a result of the declining biomass, only one of the 18 stations sampled in the area met the diatom-bloom criteria (Fig. 1). Two bloom features were sampled in 2009. In mid-June of 2009 a high chlorophyll feature developed east of Hawaii at  $\sim 26^\circ\text{N}$ ,  $146^\circ\text{W}$  (Fig. 1), but remotely sensed chlorophyll concentrations had dropped significantly by the time of sampling in mid-July (Fig. 1). However, satellite images revealed another bloom feature developing to the north of Hawaii at  $\sim 25^\circ\text{N}$ ,  $155^\circ\text{W}$  (Fig. 1). Two stations were sampled within this feature while it was still active (or developing), and both met the bloom-station criteria. This bloom will be referred to as the active bloom from PB09 to distinguish it from observations taken in the faded bloom further to the east.

Sampling consisted of CTD casts throughout the day. Pre-dawn casts (04:00–06:00 h, local time) were done to obtain samples for nutrient concentration, Chl *a* concentration,  $\text{bSiO}_2$  concentrations and  $\text{bSiO}_2$  production rates. Samples for diatom abundance and composition were taken on the rate casts or on the cast immediately before/after. On additional casts during the day, all samples were collected except those for rate measurements. Due to time constraints for sampling the second bloom region examined in 2009, rate profiles at PB09 stations 22 and 23 were conducted after 6:00 h local time, but all incubations ran 24 h to integrate through a complete photoperiod (see below). For rate measurements water samples were taken at nine depths within the euphotic zone where the percent of irradiance was determined to be 100, 59, 31, 19, 10, 6, 3.4, 0.6 and 0.1% of that just below the surface ( $\%I_0$ ). At non-rate stations fixed sampling depths (surface: i.e. 3–5 m, 10, 20, 40, 60, 80, 100, 125, 140, 160 m) were used. Seawater was collected using 12 L PVC sampling bottles on a rosette equipped with a Seabird CTD and a photosynthetically active radiation sensor to determine light attenuation. Mixed layer depths were calculated using 1-m binned CTD data based on a  $0.125 \text{ kg m}^{-3}$  change in potential density from the 0–1 m bin.

### 2.2. Nutrient, taxonomy, and biogenic particulate analysis

Dissolved nutrients were collected and analyzed using standard methods. Unfiltered seawater samples for  $[\text{Si}(\text{OH})_4]$  determination

were refrigerated at 4 °C until analysis at sea using a sensitive manual colorimetric method (Brzezinski and Nelson, 1995). Nitrate ( $< 10$  nM) and soluble reactive phosphorus ( $< 35$  nM) were also taken from sampling bottles and analyzed using both high-sensitivity methods (e.g. Church et al., 2009) and standard colorimetric methods (e.g. Villareal et al., 2012). The nutrient data are discussed in detail elsewhere (Duhamel et al., 2010, 2011; Villareal et al., 2012).

Samples for biomass and diatom-assemblage measurements were analyzed by methods used previously in subtropical-gyre regions. Seawater for biogenic (bSiO<sub>2</sub>) and lithogenic silica analysis was collected in 2.8 L polycarbonate bottles, filtered through 0.6 µm polycarbonate filters, and analyzed using the sequential NaOH–HF digestion procedure (Brzezinski and Nelson, 1995) with reactions carried out in Teflon® tubes which provide low and stable blanks (Krause et al., 2009). Lithogenic silica concentrations were very low (e.g. 3–8 nmol Si L<sup>−1</sup>) and are not discussed in detail. [Chl *a*] was determined for two size fractions:  $> 0.4$  µm (e.g. total phytoplankton community) and  $> 10$  µm (e.g. diatoms, dinoflagellates) by filtering 250 mL and 500 mL, respectively, through polycarbonate membrane filters, extracting in methanol, and quantifying fluorometrically without acidification (Welschmeyer, 1994). Samples for diatom abundance and taxonomy were preserved with formalin and enumerated using inverted microscopy (Villareal et al., 2012).

### 2.3. Measurement of biogenic silica production and export rates

Measurements of gross bSiO<sub>2</sub> production rates ( $\rho_P$ ) from each sampling depth were conducted in polycarbonate bottles (300 mL) using the radioisotope <sup>32</sup>Si. Each sample received 360 Bq of high specific activity <sup>32</sup>Si(OH)<sub>4</sub> ( $> 40$  kBq µmol Si<sup>−1</sup>) which had been cleaned of trace metals by passage through Chelex resin (BioRad). Samples were incubated on the ship deck

for 24 h in acrylic incubators, screened to the relative light level corresponding to each sample collection depth, and continuously cooled by flowing surface seawater. After incubation, all silica production rate samples were processed as described in Krause et al. (2012) and <sup>32</sup>Si activity was quantified using gas-flow proportional counting at secular equilibrium of <sup>32</sup>Si and its daughter isotope <sup>32</sup>P (Krause et al., 2011). Specific rates of silica production ( $V_b$ ) were calculated by normalizing  $\rho_P$  to [bSiO<sub>2</sub>] as in Brzezinski and Phillips (1997). The average  $V_b$  for the upper water column was calculated by vertically integrating  $V_b$  to a specific depth (e.g. 150 m) then dividing by the depth of integration.

The net bSiO<sub>2</sub> production rate ( $\rho_N$ ) was measured by the net change in biogenic silica concentrations during incubations. During PB08, two 2.8 L polycarbonate bottles were filled from each of the nine light depths sampled on rate casts and processed following the protocol from Demarest et al. (2011). Briefly, one was assigned as the initial and immediately processed, while the other was incubated for 24 h and then processed. To account for bSiO<sub>2</sub> that adsorbed to the bottle wall (Krause et al., 2010b) each sample bottle was rinsed with three aliquots of 0.2-µm-filtered seawater and the rinses passed through the same filter as the main sample. Because of the low [bSiO<sub>2</sub>] and the small net changes observed during PB08, the protocol of Krause et al. (2010b) was used during PB09, where four replicates were run as initial samples and another four incubated as final samples. The increased processing time limited experiments to four depths (59, 31, 10, and 3.4% I<sub>0</sub>). All samples were analyzed for both bSiO<sub>2</sub> and lithogenic silica, using NaOH–HF serial digestion described above, and corrected for bias assuming that 10% of the lithogenic silica dissolves during the NaOH digestion (Ragueneau and Treguer, 1994).

The export of bSiO<sub>2</sub> ( $\rho_E$ ) at 150 m and 300 m was measured on PB08 using a free-drifting Multitrap sediment trap array (e.g. Karl et al., 1996). During the PB09 cruise the combined factors of the

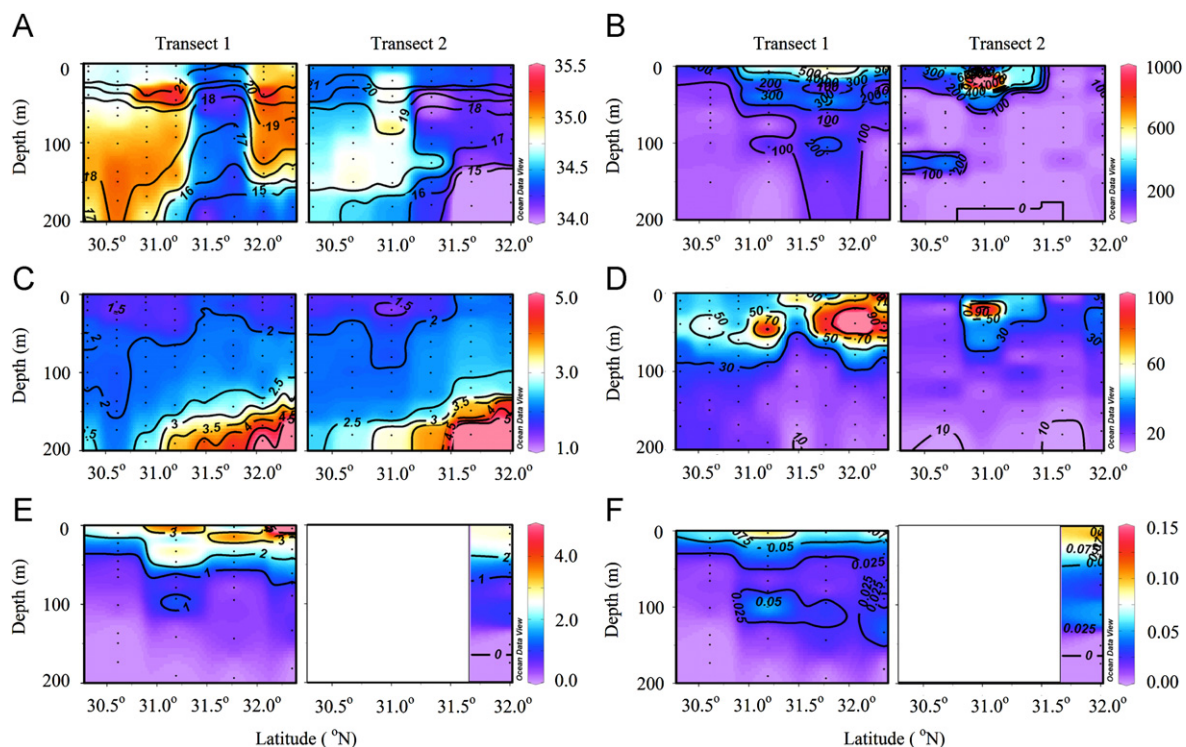


**Fig. 2.** Section plots showing hydrography, nutrients and biological properties with depth during the PB08 transects near the subtropical front. (A) Salinity (ppt) and temperature (contours, °C), (B) diatom abundance (cells L<sup>−1</sup>), (C) dissolved silicate concentration, [Si(OH)<sub>4</sub>] (µM), (D) biogenic silica concentration, [bSiO<sub>2</sub>] (nmol Si L<sup>−1</sup>), (E) biogenic silica production,  $\rho_P$  (nmol Si L<sup>−1</sup> d<sup>−1</sup>) and (F) specific biogenic silica production,  $V_b$  (d<sup>−1</sup>). The bloom station data is not shown as it was situated slightly west of transect 1 (see Fig. 1).



passage of hurricane Felicia and occupying an active bloom area for < 24 h, meant that sediment traps could not be deployed. On PB08, collector tubes fitted with entrance baffles were filled with brine ( $50 \text{ g L}^{-1}$  NaCl in  $0.2 \mu\text{m}$  filtered surface seawater) and formalin preservative was added to half the tubes. Three tubes of each type were deployed at 150 m and 300 m for approximately 5 days inside and outside of the bloom region. Samples were taken to measure the amount of  $\text{bSiO}_2$  which dissolved during deployment ( $\sim 3\%$  of particulate flux), as described in Brzezinski et al. (2011), and used to correct the total measured  $\text{bSiO}_2$  flux. Dissolution was not measured in the preserved traps, but there was no significant difference between the particulate flux in preserved and non-preserved traps deployed at the same depth and time (t-test,  $p$  values ranged 0.27–0.91 for pairwise comparisons).

### 3. Results

#### 3.1. Hydrography and nutrients

The hydrography observed during each cruise is described briefly for context; however, a more thorough description can be found in Villareal et al. (2012). During PB08, MODIS imagery revealed a bloom feature developing to the northeast of Hawaii, near the subtropical front. CTD casts in the bloom region revealed significant small-scale salinity variations in vertical profiles (Fig. 2(A), see also Villareal et al., 2012) that are characteristic

of the front (Shcherbina et al., 2009, 2010). Isotherms in the upper 100 m showed little vertical variability at most stations on both transects, but some shoaling of the isothermal surfaces was observed in the lower-salinity stations presumably associated with the front (Fig. 2A). The mixed-layer depth in the bloom region averaged  $21 \pm 7 \text{ m}$  (SD).

Prior to PB09, MODIS satellite data revealed a bloom feature near  $26^\circ\text{N}$  and  $145^\circ\text{W}$ , which began developing in mid-June. By the time of our occupation, the satellite ocean color signal faded considerably and in situ measurements indicated that the bloom had collapsed. During a zonal transect across the former bloom region the water column had less temperature and salinity variability (Fig. 3A) than was observed during the PB08 transects, and the mixed layer was  $40 \pm 13 \text{ m}$ . A smaller (areal extent) and higher [Chl  $a$ ] bloom was observed to develop closer to Hawaii, and reached the threshold bloom [Chl  $a$ ] value by 7 August. Two rate stations (Sta. 22, 23) were occupied within this active bloom on 12 August, and satellite imagery showed it collapsed by 24 August. The physical conditions were similar to those observed in the collapsed-bloom region sampled during PB09, but the mixed layer depth was deeper, 48–50 m.

Consistent with gyre conditions, the concentrations of inorganic nutrients were very low at all stations.  $[\text{Si}(\text{OH})_4]$  in the surface waters was consistently one or two orders of magnitude higher than the high-sensitivity analysis concentrations for nitrate ( $< 0.01 \mu\text{M}$ ) and soluble reactive phosphate ( $< 0.035 \mu\text{M}$ ). On PB08,  $[\text{Si}(\text{OH})_4]$  was generally  $< 2 \mu\text{M}$  in the upper 50 m and the silicicline shoaled towards the north (Fig. 2C). At the single PB08 bloom station, the

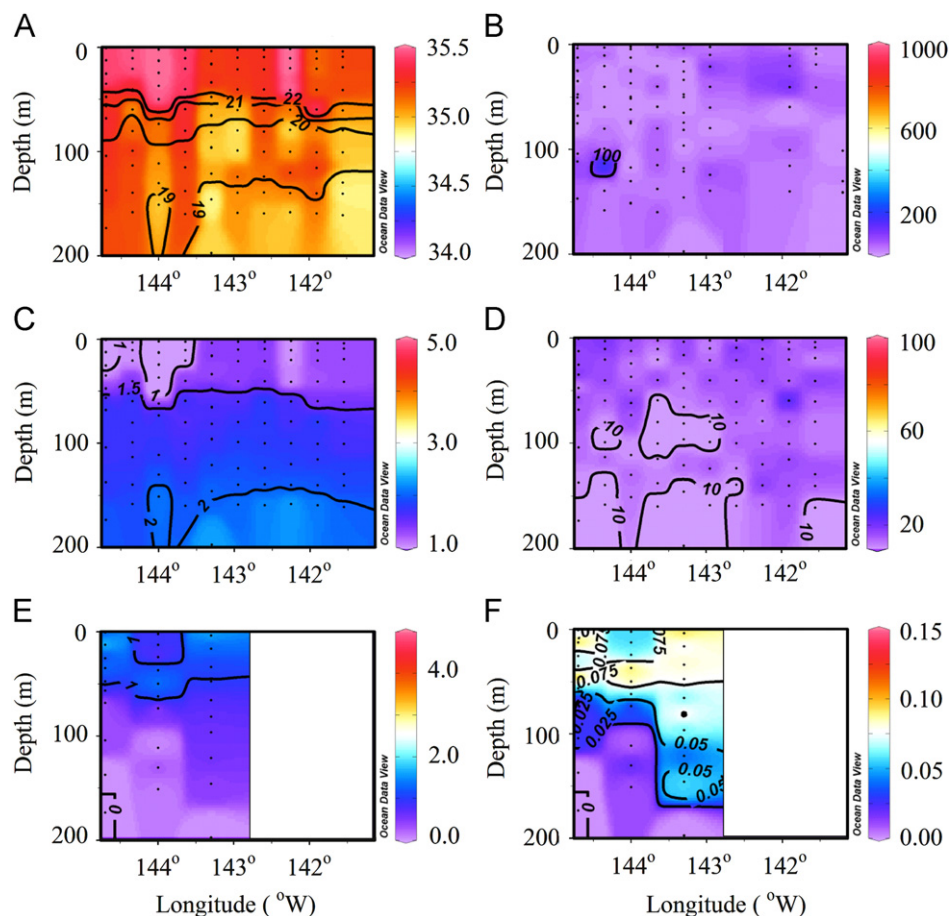


**Fig. 3.** Section plots showing hydrography, nutrients and biological properties with depth during the PB09 transect. Panels and scales are as in Fig. 2 for direct comparison. Bloom stations were located far west of this transect and are not shown (see Fig. 4). (A) Sal. (ppt) and temp. (contours,  $^\circ\text{C}$ ), (B) diatom abundance ( $\text{cells L}^{-1}$ ), (C)  $[\text{Si}(\text{OH})_4]$  ( $\mu\text{M}$ ), (D)  $[\text{bSiO}_2]$  ( $\text{nmol Si L}^{-1}$ ), (E)  $\rho_p$  ( $\text{nmol Si L}^{-1} \text{ d}^{-1}$ ), (F)  $V_b$  ( $\text{d}^{-1}$ ).

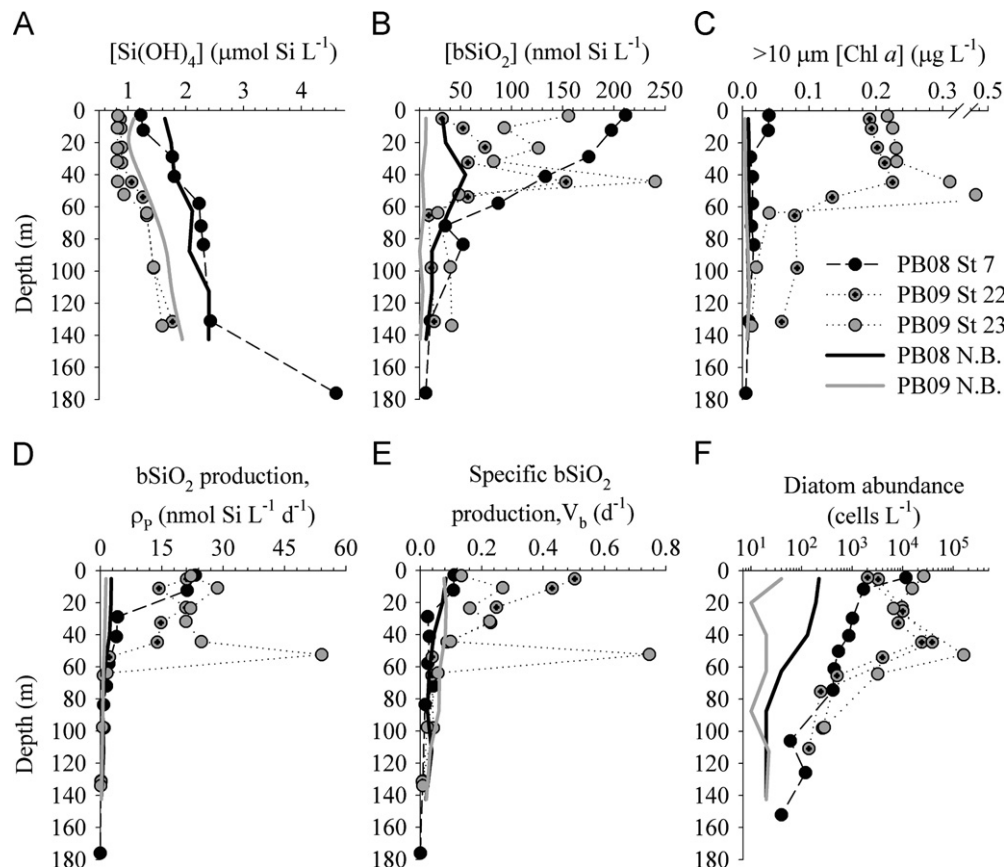


**Fig. 4.** Vertical profiles of nutrients and biological properties at the PB bloom stations. Each bloom station is distinguished by symbol type: PB08 (black), PB09 St. 22 (gray crossed), PB09 St. 23 (gray). For comparison, non-bloom (N.B.) station data were binned by depth, averaged, and plotted (depth is the midpoint of the bin) for PB08 (black line) and PB09 (gray line).

average mixed layer  $[\text{Si}(\text{OH})_4]$  showed a depletion to  $1.22 \mu\text{M}$  and the vertical gradient in silicic acid from the base of the mixed layer to the 0.1% light depth was similar to that at the northern-transect stations (Fig. 4A). Mixed-layer  $[\text{Si}(\text{OH})_4]$  at non-bloom stations was  $1.69 \pm 0.20 \mu\text{M}$ , implying a biological drawdown of  $\sim 0.5 \mu\text{M}$   $[\text{Si}(\text{OH})_4]$  in the bloom.

Dissolved silicate was consistently lower during the PB09 cruise (Fig. 3C).  $[\text{Si}(\text{OH})_4]$  in the upper 50 m on the collapsed-bloom transect was  $< 1.4 \mu\text{M}$ , and surface  $[\text{Si}(\text{OH})_4]$  was  $< 1 \mu\text{M}$  at some stations. In the active bloom, the average mixed-layer  $[\text{Si}(\text{OH})_4]$  was  $0.87 \mu\text{M}$ ,  $\sim 0.3 \mu\text{M}$  less than that at non-bloom stations (Table 1). The vertical structure in  $[\text{Si}(\text{OH})_4]$  below the mixed layer was similar at all stations during PB09 (bloom and non-bloom, Fig. 3C).

### 3.2. Particle concentrations and diatom abundance

Proxies for phytoplankton biomass showed expected low-levels outside of blooms and enhancement within blooms. We describe water-column  $[\text{Chl } a]$  (data not shown) for context and report integrated concentrations (Table 1), for a more thorough analysis of the  $[\text{Chl } a]$  dataset see Villareal et al. (2012). Total  $[\text{Chl } a]$  (i.e.  $> 0.4 \mu\text{m}$  size fraction) was typically  $0.15\text{--}0.25 \mu\text{g L}^{-1}$  in the deep chlorophyll maxima ( $\sim 80\text{--}120 \text{ m}$ ) during both years. Higher values in the overlying waters were observed in PB08 ( $0.08\text{--}0.10 \mu\text{g L}^{-1}$ ) vs. PB09 ( $< 0.08 \mu\text{g L}^{-1}$ ). At the PB08 bloom station, the total  $[\text{Chl } a]$  showed relatively minor enhancement over concentrations at non-bloom stations.  $[\text{Chl } a]$  was  $> 0.39 \mu\text{g L}^{-1}$  in the active PB09 bloom, with exceptionally high values of  $0.54$  and  $1.03 \mu\text{g L}^{-1}$  observed between  $45$  and  $55 \text{ m}$  at stations 22 and 23, respectively. On average, the  $> 10 \mu\text{m}$  fraction

was  $\leq 10\%$  of the total  $[\text{Chl } a]$  in non-bloom stations during both years. However, this larger size fraction represented  $30\text{--}40\%$  of the total  $[\text{Chl } a]$  for PB08 bloom and  $80\text{--}99\%$  at station 23 in the active PB09 bloom.

Biogenic silica concentrations were consistent with previous studies in this region.  $[\text{bSiO}_2]$  at non-bloom stations during PB08 were  $20\text{--}40 \text{ nmol Si L}^{-1}$  in the upper  $50 \text{ m}$  (Fig. 2D).  $[\text{bSiO}_2]$  maxima, up to  $100 \text{ nmol Si L}^{-1}$ , were observed between  $25\text{--}50 \text{ m}$  at some stations on both transects. At the PB08 bloom station, the  $[\text{bSiO}_2]$  surpassed  $200 \text{ nmol Si L}^{-1}$  in the surface (Fig. 4B).  $[\text{bSiO}_2]$  along the PB09 transect of the faded bloom were between  $10$  and  $20 \text{ nmol Si L}^{-1}$  with little vertical structure in the euphotic zone (Fig. 3D). But in the active PB09 bloom, the  $[\text{bSiO}_2]$  was an order of magnitude higher than at non-bloom stations, with subsurface maxima of  $153$  and  $240 \text{ nmol Si L}^{-1}$  at stations 22 and 23, respectively (Fig. 4B).

Vertical integrals of biomass measurements reveal large differences between bloom and non-bloom stations during the PB cruises. During PB08  $\int \text{Chl } a$  within the  $> 10 \mu\text{m}$  size fraction nearly doubled at the single bloom station ( $2.5 \text{ mg m}^{-2}$ ), while  $\int \text{Chl } a$  in the  $> 0.4 \mu\text{m}$  size fraction at the bloom station ( $18.3 \text{ mg m}^{-2}$ ) was similar to the non-bloom station average ( $18.8 \text{ mg m}^{-2}$ , Table 1). During PB09,  $\int \text{Chl } a$  in the  $> 10 \mu\text{m}$  size fraction was  $1.1 \text{ mg m}^{-2}$  at the non-bloom stations (includes profiles in the faded bloom) and significantly lower than the  $> 0.4 \mu\text{m}$  size fraction value ( $16.1 \text{ mg m}^{-2}$ , Table 1). But within the active PB09 bloom, substantial increases were observed in both size fractions; the  $> 10 \mu\text{m}$  and  $> 0.4 \mu\text{m}$  fractions averaged  $18.3 \text{ mg m}^{-2}$  and  $53.5 \text{ mg m}^{-2}$ , respectively (Table 1). Vertical integrals of  $[\text{bSiO}_2]$  showed relative changes similar to those of  $> 10 \mu\text{m}$   $\int \text{Chl } a$ , with significant differences between bloom and non-bloom stations. During PB08,

**Table 1**  
Mixed layer depth (MLD), dissolved silicate, biological and particulate data for the PB cruises. All integrations are to 150 m (common depth for all stations and generally shallower than the 0.1% light depth) except for the total diatoms (MLD integration).  $V_b$  is average in the upper 150 m (see Methods). Note: Integration depths for diatoms, Chl *a* and  $\text{bSiO}_2$  differ from those presented in Villareal et al. (2012), as their study focused on surface flora (i.e. 0–60 m).

Cruise	Station	Lat. (°N)	Long. (°W)	MLD (m)	MLD Ave. [Si(OH) <sub>4</sub> ] (μM)	MLD $\int$ Diatoms (10 <sup>6</sup> m <sup>-2</sup> )	Dominant diatom (%)	$\int$ bSiO <sub>2</sub> (mmol m <sup>-2</sup> )	$\int$ Chl <i>a</i> , > 0.4 μm (mg m <sup>-2</sup> )	$\int$ Chl <i>a</i> , > 10 μm (mg m <sup>-2</sup> )	$\int \rho_p$ (mmol Si m <sup>-2</sup> d <sup>-1</sup> )	Ave. $V_b$ (d <sup>-1</sup> )
PB08	1	30.00	150.00	23.3	1.90	6.27	<i>Hemiaulus</i> (69)	2.34	17.1	1.21	0.19	0.08
PB08	2	30.00	146.50	35.0	1.60	10.6	<i>Hemiaulus</i> (64)	3.06	14.4	1.10	0.19	0.05
PB08	3	32.35	140.86	11.5	1.67	4.90	<i>Hemiaulus</i> (89)	7.18	17.9	1.35	0.25	0.03
PB08	4	32.06	140.67	22.0	1.63	–	–	9.16	20.1	1.71	–	–
PB08	5	31.77	140.47	11.8	1.93	8.32	<i>Hemiaulus</i> (46)	6.16	17.7	1.26	0.18	0.03
PB08	6	31.48	140.28	15.0	1.95	–	–	3.80	21.4	1.61	–	–
PB08	a <sup>7</sup>	31.77	140.71	11.3	1.22	82.9	<i>Hemiaulus</i> (97)	12.83	18.3	2.50	0.65	0.04
PB08	8	31.67	140.92	13.0	1.39	–	–	6.85	21.7	2.01	–	–
PB08	9	31.19	140.08	27.3	1.55	8.29	<i>Hemiaulus</i> (90)	6.27	17.1	1.36	0.22	0.04
PB08	10	30.90	139.89	25.0	1.62	–	–	5.33	19.0	1.33	–	–
PB08	12	30.61	139.70	24.5	1.53	3.46	<i>Hemiaulus</i> (83)	5.48	17.3	1.35	0.10	0.02
PB08	13	30.32	139.51	14.0	1.66	–	–	5.23	19.1	1.44	–	–
PB08	14	28.75	141.25	21.3	1.50	2.26	<i>Hemiaulus</i> (89)	5.11	15.8	1.81	0.25	0.06
PB08	15	31.52	140.58	24.7	1.68	–	–	6.74	18.4	1.54	0.30	0.04
PB08	16	32.00	139.00	24.0	2.06	1.06	<i>Hemiaulus</i> (81)	3.67	19.2	1.75	0.20	0.06
PB08	17	31.67	139.33	22.0	2.10	0.25	<i>Hemiaulus</i> (99)	2.79	20.8	1.63	–	–
PB08	18	31.33	139.67	26.0	1.68	10.6	<i>Hemiaulus</i> (98)	3.69	19.9	1.63	–	–
PB08	19	31.00	140.01	21.0	1.49	12.5	<i>Hemiaulus</i> (97)	5.08	20.1	1.69	–	–
PB08	20	30.67	140.34	12.0	1.58	4.06	<i>Hemiaulus</i> (99)	2.66	19.4	1.52	–	–
PB08	21	30.33	140.67	22.0	1.60	3.93	<i>Hemiaulus</i> (~100)	~	20.2	1.59	–	–
PB09	1	20.50	153.69	34.5	1.19	3.79	<i>Mastogloia</i> (73)	2.12	21.0	1.88	0.15	0.07
PB09	2	25.20	147.00	28.0	1.04	1.01	<i>Mastogloia</i> (36)	1.80	16.5	1.37	–	–
PB09	b <sup>3</sup>	26.10	144.70	43.0	0.99	0.99	<i>Mastogloia</i> (67)	2.11	17.7	1.09	0.10	0.05
PB09	b <sup>4</sup>	26.10	144.35	37.0	1.02	0.49	<i>Mastogloia</i> (64)	1.91	18.8	1.71	–	–
PB09	b <sup>7</sup>	26.10	144.00	49.0	0.86	0.25	<i>Mastogloia</i> (49)	2.03	4.68	0.31	0.10	0.05
PB09	b <sup>8</sup>	26.10	143.65	42.0	1.03	0.69	<i>Hemiaulus</i> (34)	1.57	16.0	0.95	–	–
PB09	b <sup>11</sup>	26.10	143.30	43.5	1.32	0.56	<i>Mastogloia</i> (74)	1.77	16.4	0.93	0.12	0.07
PB09	b <sup>12</sup>	26.10	142.95	8.0	1.34	0.20	<i>Mastogloia</i> (~100)	1.80	15.3	0.80	–	–
PB09	13	25.48	143.00	36.8	1.02	1.27	<i>Hemiaulus</i> (55)	1.99	14.7	0.93	0.13	0.06
PB09	b <sup>15</sup>	26.10	142.60	40.0	1.37	–	–	2.04	15.0	0.76	–	–
PB09	b <sup>16</sup>	26.10	142.25	58.0	1.02	–	–	2.24	17.1	1.20	–	–
PB09	b <sup>17</sup>	26.10	141.90	34.5	1.28	2.46	<i>Mastogloia</i> (56)	2.34	20.9	1.39	–	–
PB09	b <sup>18</sup>	26.10	141.55	48.0	1.26	0.89	<i>Mastogloia</i> (86)	2.05	15.2	0.94	–	–
PB09	20	27.50	142.00	37.0	1.30	–	–	2.54	15.7	1.00	–	–
PB09	21	23.50	140.00	58.6	1.30	6.96	<i>Chaetoceros</i> (74)	1.69	17.6	1.18	0.10	0.06
PB09	a,c <sup>22</sup>	25.10	154.70	47.7	0.91	509	<i>Mastogloia</i> (98)	6.13	63.3	18.05	0.91	0.16
PB09	a,c <sup>23</sup>	25.18	154.60	52.7	0.82	2410	<i>Mastogloia</i> (99)	9.19	43.7	18.53	1.74	0.17

<sup>a</sup> Bloom stations (i.e. fulfilled data-based criteria).

<sup>b</sup> Faded bloom stations (PB09; 26°N, 145°W).

<sup>c</sup> Integration depth (0.1% $I_0$ ) was only 131 and 134 m for stations 22 and 23, respectively.

the non-bloom  $\int$  bSiO<sub>2</sub> averaged 40% of the bloom station value (13.3 mmol Si m<sup>-2</sup>, Table 1). Similarly, the non-bloom  $\int$  bSiO<sub>2</sub> in PB09 was only 26% of the  $\int$  bSiO<sub>2</sub> at the two active bloom stations during PB09 (7.7 mmol Si m<sup>-2</sup>, Table 1).

Diatom abundance and species dominance differed between cruises. During PB08, *Hemiaulus hauckii* was the numerically dominant diatom at all stations (Table 1). The vertical structure in diatom abundance (Figs. 2B, 3B and 4F) was similar to that for  $\int$  bSiO<sub>2</sub> (Figs. 2D, 3D and 4B) and > 10 μm [Chl *a*] (Fig. 4C). Surface maximums of ~250 cells L<sup>-1</sup> were observed during the PB08 transects, with abundances < 50 cells L<sup>-1</sup> persisting deeper than 50 m (Fig. 2B). Diatom abundance increased to > 10,000 cells L<sup>-1</sup> in the surface at the bloom station, with > 100 cells L<sup>-1</sup> at depths shallower than 60 m (Fig. 4F). The integrated diatom abundance within the mixed-layer varied by an order of magnitude between non-bloom (5.9 × 10<sup>6</sup> cells m<sup>-2</sup>) and bloom stations (8.2 × 10<sup>7</sup> cells m<sup>-2</sup>, Table 1). *M. woodiana* dominated abundance at 11 of the 14 stations where abundance data was obtained during PB09, with *H. hauckii* and *Chaetoceros* spp. being most abundant diatoms at the other stations (Table 1). Non-bloom station cell abundance was very low, e.g. < 50 cells L<sup>-1</sup>,

with little vertical structure (Fig. 3B). Within the active bloom, *M. woodiana* accounted for 98% of total diatom abundance, despite maximum numerical abundances for all diatom genera being observed in this bloom (Table 1). Maximum diatom cell abundances in the station-22 mixed layer were 38,000 cells L<sup>-1</sup>, and maximum mixed-layer abundances were higher at station 23 (159,000 cells L<sup>-1</sup>, Fig. 4F). The mixed-layer integrated diatom abundance at non-bloom stations during PB09 (1.1 × 10<sup>6</sup> cells m<sup>-2</sup>) was three orders of magnitude lower than at the active bloom stations (1.4 × 10<sup>9</sup> cells m<sup>-2</sup>; Table 1).

### 3.3. Biogenic silica production and export rates

Gross biogenic silica production rates ( $\rho_p$ ) varied by an order of magnitude between bloom and non-bloom stations. Surface  $\rho_p$  ranged between 2–5 nmol Si L<sup>-1</sup> d<sup>-1</sup> at non-bloom stations during PB08 (Fig. 2E) and increased to > 20 nmol Si L<sup>-1</sup> d<sup>-1</sup> at the bloom station (Fig. 4D). Vertical trends in  $\rho_p$  below 50 m were similar in and out of the bloom area, with rates declining from < 1 nmol Si L<sup>-1</sup> d<sup>-1</sup> at 50 m to analytically zero at 175 m, indicating that the full vertical extent of  $\rho_p$  in the water column

was sampled (Fig. 2E). At PB09 non-bloom stations, only two samples (out of 59) had rates  $> 2 \text{ nmol Si L}^{-1} \text{ d}^{-1}$ . Rates in the upper 50 m were generally  $1.2\text{--}1.8 \text{ nmol Si L}^{-1} \text{ d}^{-1}$  and below 50 m, deep  $\rho_P$  declined to rates similar to rates observed in PB08 (Fig. 3E). Within the active PB09 bloom,  $\rho_P$  values were  $> 15 \text{ nmol Si L}^{-1} \text{ d}^{-1}$  throughout the upper 50 m, with a subsurface maximum of  $54 \text{ nmol Si L}^{-1} \text{ d}^{-1}$  (Fig. 4D). Deeper than 60 m,  $\rho_P$  at the active bloom stations were nearly identical to those rates measured at non-bloom stations. Vertical integrals of  $\rho_P$  ( $\int \rho_P$ ) demonstrate the strong disparity between bloom and non-bloom rates. Non-bloom station average  $\int \rho_P$  during PB08 was 32% of the bloom-station rate ( $0.65 \text{ mmol Si m}^{-2} \text{ d}^{-1}$ , Table 1). A larger disparity was observed in PB09, as the non-bloom average  $\int \rho_P$  was only 9% of the active bloom rate ( $1.33 \text{ mmol Si m}^{-2} \text{ d}^{-1}$ ).

As with  $\rho_P$  [ $\text{bSiO}_2$ ], and diatom abundance, specific uptake rate  $V_b$  was generally highest in the upper water column and declined to analytical zero values at the  $0.1\%I_0$  isolume (Figs. 2F, 3F and 4E). During PB08,  $V_b$  in the upper 15 m were  $\sim 0.05\text{--}0.08 \text{ d}^{-1}$  at non-bloom stations (Fig. 2F), but at the bloom station  $V_b$  in the upper 15 m was  $\sim 0.11 \text{ d}^{-1}$  (Fig. 4E), implying doubling times of  $\sim 6$  and  $\sim 10$  days inside and outside bloom, respectively. Vertically weighted average  $V_b$  within the upper 150 m showed no difference between the non-bloom ( $0.05 \text{ d}^{-1}$ ) and bloom ( $0.04 \text{ d}^{-1}$ ) rates (Table 1), indicating an average doubling time for  $\text{bSiO}_2$  in the upper 150 m of approximately two weeks during the PB08 cruise.  $V_b$  on the faded-bloom transect during PB09 was  $> 0.05 \text{ d}^{-1}$  in the upper 50 m at two stations and values were  $\geq 0.05 \text{ d}^{-1}$  throughout the upper 150 m at the easternmost station (Fig. 3F). At the active-bloom stations during PB09,  $V_b$  averaged  $\sim 0.35 \text{ d}^{-1}$  in the upper 10 m with a maximum of  $0.75 \text{ d}^{-1}$  at the base of the mixed layer ( $\sim 50 \text{ m}$ , Fig. 4E); the latter infers a doubling time of  $< 1$  day. For PB09, the vertically averaged  $V_b$  within the active bloom ( $0.17 \text{ d}^{-1}$ ) was nearly three-fold higher than for non-bloom stations ( $0.06 \text{ d}^{-1}$ ), implying doubling times of 4 and 11 days for bloom and non-bloom stations, respectively.

The net production of biogenic silica ( $\rho_N$ ) is defined as the difference between  $\rho_P$  and gross silica dissolution, and thereby represents an upper limit for  $\text{bSiO}_2$  export. Because  $\rho_N$  was not sampled at every rate station during PB08, we do not have a measurement at the single bloom station. When integrated within the mixed layer,  $\int \rho_N$  was positive at three stations (Fig. 5). Integration to deeper depths (e.g.  $3.4\%I_0$  and  $0.1\%I_0$ ) caused  $\int \rho_N$  to become negative, indicating that within the euphotic zone the dissolution of  $\text{bSiO}_2$  exceeded its rate of production. During PB09, replication allowed for constraints on the variability in the estimates of  $\int \rho_N$  (Fig. 5B). Nearly all stations showed positive  $\int \rho_N$  over the mixed layer and often between the surface and the  $3.4\%I_0$  isolume (Fig. 5), but only in the active bloom (stations 22, 23, Fig. 5) was  $\int \rho_N$  statistically different from zero (i.e. production of  $\text{bSiO}_2$  exceeded its loss from dissolution) for the mixed layer and to the  $3.4\%I_0$  isolume integrals. Considering the variability among replicated samples during PB09,  $\int \rho_N$  measured during PB08 were unlikely to be statistically different from zero. These results suggest that the outside of bloom stations, silica production and dissolution were approximately in balance leading to no or very little net silica production (i.e.  $\int \rho_N \approx 0$ ) within the mixed layer.

Due to inclement weather, no sediment trap deployments were made during PB09; however, we can make comparisons between bloom and non-bloom regions for  $\text{bSiO}_2$  flux ( $\rho_E$ ) during PB08. Samples with and without formalin showed no statistically significant difference in the measured  $\rho_E$  (t-test, p values ranged  $0.27\text{--}0.91$ ), and we report the pooled mean  $\pm$  SD from both trap types.  $\rho_E$  at 150 m within the bloom area was higher than that observed outside the bloom ( $0.27 \pm 0.05 \text{ mmol Si m}^{-2} \text{ d}^{-1}$  vs.

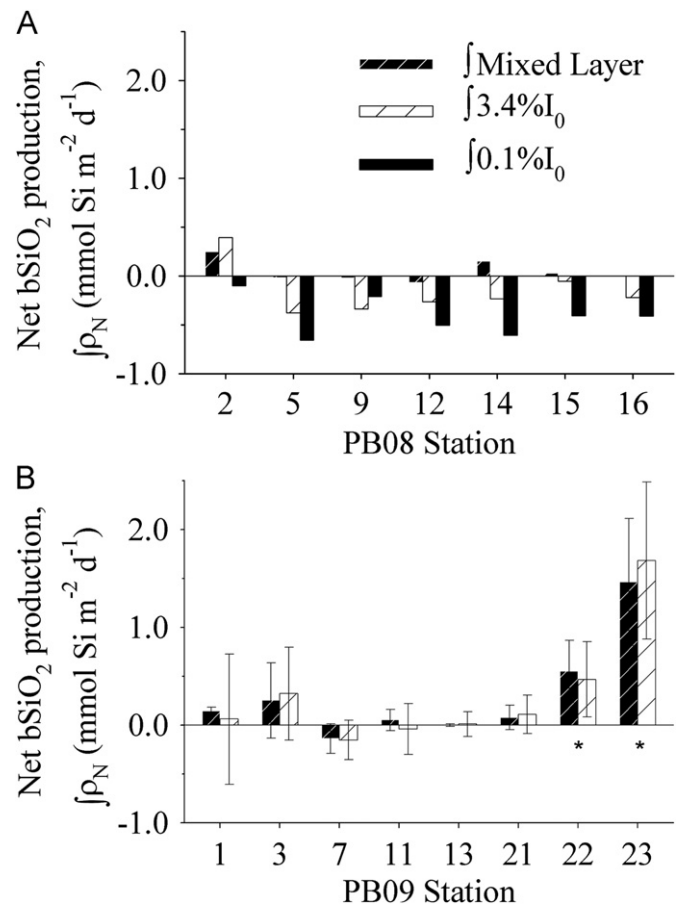


Fig. 5. The net production of  $\text{bSiO}_2$  ( $\rho_N$ ) during (A) PB08 and (B) PB09. Bars represent vertical integrals based either in the mixed layer or to a specific light depth. \*Indicates bloom station during PB09, the PB08 bloom station was not sampled. Error bars are propagated from the measured variance in the replicates, and summed with depth.

$0.17 \pm 0.03 \text{ mmol Si m}^{-2} \text{ d}^{-1}$ ). Unexpectedly,  $\rho_E$  at 300 m in the bloom area was  $0.36 \pm 0.03 \text{ mmol Si m}^{-2} \text{ d}^{-1}$ ,  $\sim 33\%$  higher than  $\rho_E$  at 150 m in the bloom, and was four-fold higher than 300-m  $\rho_E$  outside the bloom ( $0.09 \pm 0.01 \text{ mmol Si m}^{-2} \text{ d}^{-1}$ ).

## 4. Discussion

### 4.1. Siliceous biomass and silica production during summer in the NPSG

The blooms sampled during the PB cruises are similar to summer-period stocks and rates observed previously in this region. On zonal transects along  $\sim 25^\circ\text{N}$  and  $31^\circ\text{N}$  in NPSG during summer, Brzezinski et al. (1998) observed a  $\int \text{bSiO}_2$  range of  $2\text{--}18 \text{ mmol Si m}^{-2}$  (Fig. 6A), but by our diatom-bloom criteria only one bloom station was sampled during their cruises. Between 1997 and 2009, summer blooms occurred most years at station ALOHA, elevating  $\int \text{bSiO}_2$  by  $\sim 50\%$  above the non-summer average ( $2.5 \text{ mmol Si m}^{-2}$ ; Brzezinski et al., 2011). The PB08 bloom-station  $\int \text{bSiO}_2$  (Table 1) was similar to the highest values observed in all 12 years of  $\text{bSiO}_2$  data at station ALOHA, but about  $33\%$  lower than the highest integrals reported by Brzezinski et al. (1998) (Fig. 6A). Similarly, the  $\int \text{bSiO}_2$  at the PB09 active bloom stations (Table 1) was comparable to the highest values observed in the ALOHA record (Fig. 6A). Non-bloom station  $\int \text{bSiO}_2$  during the PB cruises (Table 1) was also similar to values



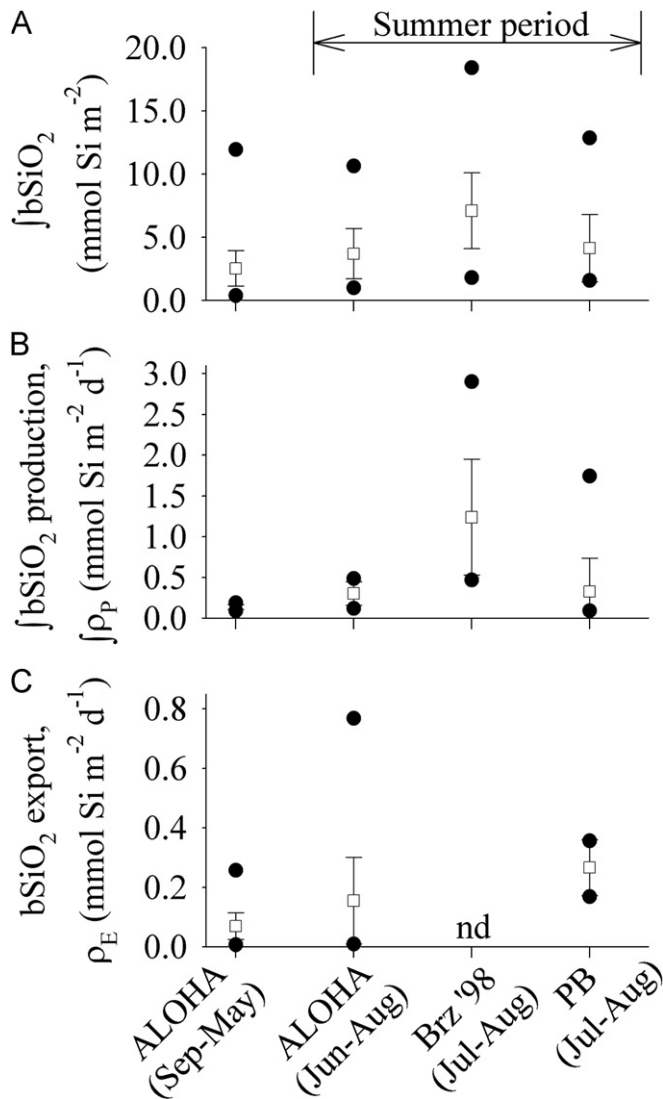


**Fig. 6.** Comparison of (A)  $\int bSiO_2$ , (B)  $\int \rho_p$ , and (C) 150-m  $bSiO_2$  export in the NPSG. The square symbols and error bars are the average and standard deviation, respectively, filled symbols represent data range. Data are arranged by non-summer (September through May) and summer (bloom season, June through August) months. Data is from Brzezinski et al. (2011) (station ALOHA), Brzezinski et al. (1998) (transects north of ALOHA during August 1995, July 1996), and this study; “nd” indicates no data. The PB08 bloom export value at 300 m is averaged with the flux values at 150 m from in and out of the bloom area (total of three data points).

during previous studies in this region (Fig. 6A). Combining our data with the previous data at station ALOHA and from transects by Brzezinski et al. (1998) shows that the magnitude of  $\int bSiO_2$  during the summer season does not appear to increase from the gyre interior (near ALOHA) to the northeastern boundary (near the subtropical front).

Reports of biogenic silica production rates in the NPSG are limited. Brzezinski et al. (1998) reported  $\int \rho_p$  between 0.5 and 2.9 mmol Si m<sup>-2</sup> d<sup>-1</sup> (average 1.2 mmol Si m<sup>-2</sup> d<sup>-1</sup>) during their summer cruises in the mid-1990s (Fig. 6B). This range and mean were significantly higher than that observed recently at station ALOHA, where non-summer  $\int \rho_p$  ranged between 0.1–0.2 mmol Si m<sup>-2</sup> d<sup>-1</sup> and summer values averaged 0.4 mmol Si m<sup>-2</sup> d<sup>-1</sup> (Fig. 6B; Brzezinski et al., 2011).  $\int \rho_p$  at the three PB bloom stations was higher than at ALOHA during the summer (Brzezinski et al., 2011) and they were similar to the mean rate reported for all stations by Brzezinski et al. (1998) (Fig. 6B). One

other report of biogenic silica production rates in this region was for *Rhizosolenia* mats during the summer months (Shipe et al., 1999). Shipe et al. (1999) estimated that *Rhizosolenia* mat production was up to ~0.3 mmol Si m<sup>-2</sup> d<sup>-1</sup> in the upper 150 m. This rate surpasses nearly all non-bloom stations during the PB cruises (Table 1) and reinforces Shipe et al. (1999) conclusions that *Rhizosolenia* mats are an important overlooked source of silica production in this region.

#### 4.2. Comparison to other open-ocean diatom blooms

Even under bloom conditions, the diatom biomass in the NPSG is lower than coastal zones (Brzezinski et al., 1997, 2003; Shipe and Brzezinski, 2001) or the Southern Ocean/Antarctica (Nelson et al., 1991) and this results in significantly lower rates of  $bSiO_2$  production (Table 2). Consequently, NPSG gross rates are low and similar in magnitude to other subtropical gyres. However, the elevated rates observed in the PB blooms are comparable to those observed in subtropical-gyre mesoscale features, where intensified vertical nutrient supply enhances phytoplankton rate processes (e.g. McGillicuddy et al., 1998). NPSG blooms are distinct for being spatially larger (Table 2) and for occurring without significant enhancement of macronutrients by obvious mesoscale processes. In the Sargasso Sea, Krause et al. (2010b) observed greatly enhanced  $\int bSiO_2$ ,  $\int \rho_p$  and  $\int \rho_N$  in a mode-water eddy (MWE), the same eddy type harboring the enhanced diatom community described by McGillicuddy et al. (2007). While  $\int bSiO_2$  was higher in the MWE than at all PB stations,  $\int \rho_p$  was similar and the total amount of  $bSiO_2$  produced in this MWE may have been similar to that observed in the PB09 bloom (Table 2). But  $\int \rho_N$  was nearly 3-fold higher in the PB09 bloom compared to the MWE. Eddies have also been observed to have enhanced diatom biomass relative to normal (e.g. non-bloom) conditions in the NPSG (Benitez-Nelson et al., 2007; Fong et al., 2008), but direct comparison with the PB blooms is problematic since no measurements of  $\int bSiO_2$  and silica production were made during these studies. However, Benitez-Nelson et al. (2007) did report a 150-m  $\rho_e$  of 0.43 mmol Si m<sup>-2</sup> d<sup>-1</sup> in an NPSG cyclonic eddy (i.e. “Cyclone Opal”), this value is only 20% higher than the 300-m  $\rho_e$  measured in PB08 bloom region (Fig. 6C).

Compared to other diatom blooms examined to date, the PB09 bloom appeared to have lower proportional losses of biogenic silica due to silica dissolution. The ratio of net  $bSiO_2$  accumulation relative to the gross rate ( $\int \rho_N / \int \rho_p$ ) is equivalent to the statistic 1—D:P, a diagnostic of fraction of “new” silica production (Brzezinski et al., 2003) (D:P is the ratio of gross silica dissolution to gross silica production). In the PB09, the 1—D:P in the active bloom was 0.77, this is higher than other blooms in subtropical gyres (e.g. 0.66; Krause et al., 2010b) and is similar to bloom values observed in high-diatom biomass systems including the Gulf Stream Warm Core Rings, Antarctic Polar Front, and the Amazon River Plume (see Fig. 4 in Brzezinski et al., 2003). Thus, in the active PB09 bloom, the much lower proportional loss of  $bSiO_2$  due to dissolution allows for a higher fraction of  $\rho_p$  to result in  $\int bSiO_2$  accumulation and potentially export.

#### 4.3. Bloom drivers

The summer blooms in the NPSG have been shown to be quantitatively significant in terms of their effect on the annual export of particulate organic matter to the ocean interior (Scharek et al., 1999b; Dore et al., 2008; Karl et al., 2012); however, a consensus view as to what is driving blooms during this period has yet to be realized. A companion study suggested that Si was not limiting to diatom growth during these blooms (Krause et al., 2012); therefore, input of Si can be eliminated as a potential

**Table 2**

Estimates for the amount of bSiO<sub>2</sub> produced by the individual blooms sampled in 2008 and 2009 (active bloom), and for the bSiO<sub>2</sub> produced during the bloom season (June–October) in three latitude bins, assuming a duration of 10 days (see Fig. 7). For comparison, we have included bSiO<sub>2</sub> produced in other regions using published bloom rates and also assuming a 10-day duration.

Bloom or Region	$\int \rho_P$ (mmol Si m <sup>-2</sup> d <sup>-1</sup> )	Duration (days)	<sup>a</sup> Bloom area (km <sup>2</sup> )	bSiO <sub>2</sub> produced (Gmoles)	Reference
PB08 bloom	0.65	16	100,000	1.04	This study
PB09 bloom	1.33	16	30,000	0.64	
NPSG 2008 bloom season					
20–25°N	0.99	10	234,798	2.32	This study
25–30°N	0.99	10	114,425	1.13	
30–35°N	0.99	10	758,114	7.51	
NPSG 2009 bloom season					This study
20–25°N	0.99	10	15,052	0.15	
25–30°N	0.99	10	57,156	0.57	
30–35°N	0.99	10	386,566	3.83	Krause et al., 2010b Brzezinski et al., 1997, 2003 Shipe and Brzezinski, 2001 Nelson et al., 1991
Sargasso sea: Mode-water eddy	0.98	10	24,200	0.24	
Monterey Bay	60	10	1200	0.72	
Santa Barbara channel	40	10	4200	1.68	Nelson et al., 1991
Ross Sea polynya	34	10	<sup>b</sup> 160,000	54.4	

<sup>a</sup> Bloom rate is assumed over the **entire** regional area.

<sup>b</sup> Average open water area (October–May) over nine years (Arrigo and van Dijken, 2004).

bloom driver. The increase in available N by enhanced nitrogen fixation has been suggested to be a mechanism which facilitates blooms in the NPSG (e.g. Wilson, 2003; Dore et al., 2008); such that blooms of diazotrophs or DDAs would be regulated more by nutrients such as phosphorus and iron (e.g. Calil et al., 2011). This did not seem to be the case during PB08. A study of phosphorus cycling by Duhamel et al. (2010) found little evidence of P limitation during PB08 leading to the suggestion that the autotrophs present were mainly limited by N, thus giving direct advantage to organisms capable of N<sub>2</sub> fixation. This is consistent with the finding that *H. hauckii*, a DDA, dominated the PB08 diatom silica biomass and silica production rates (Krause et al., 2012). However, N<sub>2</sub> fixation rates measured on the cruise were quite low. Watkins-Brandt et al. (2011) report the highest N<sub>2</sub> fixation rates on this cruise to be  $\sim 2$  nmol N L<sup>-1</sup> d<sup>-1</sup>, with most values being  $\leq 1$  nmol N L<sup>-1</sup> d<sup>-1</sup>. Considering an average diatom Si:N of 1:1 (Brzezinski, 1985) and the maximizing assumption that all measured N<sub>2</sub> fixation was solely by DDAs, then the measured N<sub>2</sub> fixation rates by Watkins-Brandt et al. (2011) could potentially support most silica production at non-bloom stations, but < 10% of silica production rates measured at the PB08 bloom station.

The dominant diatom in the active bloom on PB09, *M. woodiana*, is not a DDA and thus does not benefit directly from N<sub>2</sub> fixation. *M. woodiana* has been observed on multiple occasions to be a numerically dominant diatom in NPSG blooms (see Table 1 in Dore et al., 2008). Despite its small size, it also has been observed to be high abundance in local sediment traps (Scharek et al., 1999a, 1999b), possibly because of its ability to form large aggregates (Villareal et al., 2012). Both *M. woodiana* and DDAs are part of the same near-surface flora (Venrick, 1988), suggesting that *M. woodiana* benefits from an indirect linkage with coexisting DDAs where food web processes, or direct N excretion, transfer N from DDAs to non-nitrogen fixers, but the role of such processes in bloom initiation and/or development remains unclear (Villareal et al., 2012).

Other mechanisms that may drive blooms are physical, including mesoscale features (Church et al., 2009) and fronts (Calil and Richards, 2010). In a synthesis of four blooms sampled in the northeastern sector of the NPSG (including the two blooms reported here), Wilson et al. (in review) suggest that bloom development requires a subsurface stratification minimum intersecting the nutricline and that this is close to the base of the mixed layer. However, this assumes that biological productivity in blooms is driven by N<sub>2</sub> fixation (i.e. solitary/colonial diazotrophs

or DDA) making biological production limited by P availability. Wilson (2011) recently presented a hypothesis to explain blooms occurring to the northeast of Hawaii near the subtropical front where internal waves, generated at the Hawaiian islands, propagate to the northeast and break near a “critical latitude” (e.g. 30°N), thereby enhancing vertical mixing across the nutricline. The PB08 bloom was located very near the “critical latitude.”

#### 4.4. Bloom dynamics

Multiple lines of evidence suggest the PB08 bloom region was sampled while in a declining state. The MODIS satellite data showed that surface [Chl *a*] had started declining in this feature prior to our sampling. The bloom had [Chl *a*] above the 0.12  $\mu\text{g L}^{-1}$  threshold through at least 8 July 2008, although due to cloud coverage much of the feature was obscured from MODIS during its decline. The bloom station was sampled on 9 July; thus, most of our stations were sampled after the bloom was below the ocean color bloom threshold. Evidence of bloom decline was also apparent by a lack of significant differences in  $V_b$  between the PB08 bloom and those at some non-bloom stations (Figs. 2 and 3, Table 1), indicating low diatom activity in the declining bloom. Lastly, there was a lack of vertical attenuation of  $\rho_E$  in the bloom. The export at 300 m was 33% higher than that at 150 m, whereas outside the bloom the bSiO<sub>2</sub> flux at 300 m was half of the flux at 150 m. Given the temporal lag for particles exported at 150 m to reach 300 m, the increase in flux with depth suggests that a large pulse of silica export occurred prior to our occupation.

In contrast to the PB08 bloom, nearly every measurement taken supports that the active PB09 bloom was sampled in a state of rapid autotrophic biomass accumulation. The MODIS data indicates that stations 22 and 23 were sampled at the peak biomass achieved by this bloom (Villareal et al., 2012). The  $\rho_P$  and  $V_b$  observed in this bloom were the highest of all stations during both PB cruises and were comparable to the highest rates observed at station ALOHA during two years of study (2008–2009; Brzezinski et al., 2011). The high specific production rates imply doubling-time estimates within the PB09 active bloom to be < 1–2 days in the upper 55 m, relative to the 10–14 day doubling times elsewhere. This evidence suggests a highly dynamic diatom community, despite the predominant condition of very low [NO<sub>3</sub>], [SRP] (i.e. no different than non-bloom stations), which was still in a state of positive net bSiO<sub>2</sub> production during our sampling, notwithstanding the even lower [Si(OH)<sub>4</sub>] than non-bloom station (presumably from biological drawdown).

A distinction among the three bloom stations sampled on the PB cruises is the shift in numerical dominance by different diatom genera among blooms and their implied contribution to silicon dynamics. Recently, we used a biovolume scaling approach (sensu Conley et al., 1989) to determine the Si quota of the dominant diatoms in the PB blooms to estimate which diatom species likely dominated  $\rho_P$  and the community  $V_b$  (Krause et al., 2012). We observed that *H. hauckii* and *M. woodiana* dominated the PB08 and active PB09 blooms, respectively, and they likely dominated  $\rho_P$  due to the combined effects of each group having the highest contribution to [bSiO<sub>2</sub>] and highest net growth rates, compared to the other diatoms present. Thus, in these blooms it appears that numerical dominance by a particular diatom group also resulted in those groups having the most significant role in local silicon biogeochemistry. Such a condition is not always true among diatom assemblages, as a recent analysis in the eastern equatorial Pacific suggested that up to 40% of the  $\int \rho_P$  in the euphotic zone was done by diatoms representing < 10% of the total abundance (Krause et al., 2010a).

The export of biogenic silica in the PB08 bloom was significant in the context of the regional dataset. Biogenic silica flux at 150 m has been regularly sampled by the HOT program since 1997 (Brzezinski et al., 2011) where  $\rho_E$  is  $\sim 0.07$  mmol Si m<sup>-2</sup> d<sup>-1</sup> and  $\sim 0.13$  mmol Si m<sup>-2</sup> d<sup>-1</sup> during non-summer and summer months, respectively (Fig. 6C). During the PB08 cruise,  $\rho_E$  within and outside of the bloom region were both enhanced, relative to average rates observed at station ALOHA (Fig. 6C). The 300-m  $\rho_E$  of 0.36 mmol Si m<sup>-2</sup> d<sup>-1</sup> within the PB08 bloom area is higher than all but two of the 87 cruise values reported for 150 m  $\rho_E$  at ALOHA since 2001 (Brzezinski et al., 2011) and was 85% of the 150-m  $\rho_E$  observed at in a regional cyclonic eddy ("Cyclone Opal") which harbored significantly enhanced diatom biomass (Benitez-Nelson et al., 2007). Under steady-state conditions, the  $\int \rho_N$  measurement sets an upper limit for export. At most stations, positive  $\int \rho_N$  was observed in the mixed layer, with increasingly negative values for deeper integral depths (Fig. 5). Such biomass accumulation, and export potential, in the mixed layer, suggests that diatoms in the NPSG may operate in reverse of the classical two-layer model (Dugdale, 1967; Eppeley et al., 1973), where export originates in the deeper layer from phytoplankton having adequate nutrients but are limited by light.

During the PB cruises we can adequately resolve differences in net production between the bloom and non-bloom stations but the method has high uncertainty due to natural variability in bSiO<sub>2</sub> replicates. At station ALOHA, an average of 54% of total integrated silica production is available for export (i.e. net production) (Brzezinski et al., 2011); however, the absolute export rates were low (see previous paragraph). With the high uncertainty in the  $\int \rho_N$  measurement, such a small positive signal in  $\int \rho_N$  (inferred by the station ALOHA dataset) at non-bloom stations cannot be resolved. Only in the active PB09 bloom was  $\int \rho_N$  positive and statistically different from zero, suggesting that during this bloom there was an increased decoupling between production and dissolution of silica, relative to that observed under non-bloom conditions, this decoupling lead to higher net accumulation of biomass and high export potential. The observation that *M. woodiana* formed visible aggregates in this bloom (Villareal et al., 2012) provides a mechanism to enhance the settling rate of these diatoms, relative to the rate for single cells, thereby enabling *M. woodiana* to be important in export (*M. woodiana* and *H. hauckii* numerically dominate diatom flux at ALOHA during summer; Scharek et al., 1999b). The PB09 bloom  $\int \rho_N$  implies a maximum potential for export of 1.1 mmol Si m<sup>-2</sup> d<sup>-1</sup>, which  $\sim 40\%$  higher than the highest  $\rho_E$  observed in this region (Fig. 6C), and consistent with diatom export during summer blooms being important to regional carbon export (Karl et al., 2012).

#### 4.5. The potential summer bloom effect on the annual Si budget in the NPSG

During 2008 and 2009 at station ALOHA, blooms accounted for 29% of annual  $\int \rho_P$  (Brzezinski et al., 2011). This percentage is based on average daily rates of 0.4 mmol Si m<sup>-2</sup> d<sup>-1</sup> during two summer-period blooms. Incorporating the  $\int \rho_P$  from the active PB09 bloom ( $\sim$  same latitude as ALOHA; Fig. 1) into the Brzezinski et al. (2011) average, increases the bloom-average  $\int \rho_P$  from 0.4 mmol Si m<sup>-2</sup> d<sup>-1</sup> to 0.63 mmol Si m<sup>-2</sup> d<sup>-1</sup> or by 50%. Based on the limited number of diatom blooms sampled at or near station ALOHA, the contribution of blooms to annual silica production rates calculated by Brzezinski et al. (2011) may be conservative.

Calculating the contribution of blooms to annual budgets requires their total silica production, frequency, and areal extent. Bloom frequency and areal extent are best obtained from satellite ocean color recognizing the limitations of linking DDA-diatom blooms to ocean color (Villareal et al., 2011, 2012). The PB08 bloom had remotely-observed [Chl *a*] of  $> 0.12$   $\mu\text{g L}^{-1}$  over an average area of 100,000 km<sup>2</sup>. The active PB09 bloom had significantly higher silica production but covered only 30,000 km<sup>2</sup>. Both blooms persisted  $\sim 16$  days but during this time period cloud cover sometimes obscured the bloom, introducing a likely error of at least a few days. Using the  $\int \rho_P$  for the bloom stations (e.g. PB09 average 1.33 mmol Si m<sup>-2</sup> d<sup>-1</sup>), we estimate that the PB08 and PB09 blooms produced 1.04 and 0.64 Gmoles of bSiO<sub>2</sub>, respectively (Table 2). For comparison, non-bloom rates expressed over this same area and duration would yield 0.21 and 0.12 Gmoles of bSiO<sub>2</sub> for PB08 and PB09, respectively. Due to their tremendous areal extent, these blooms also are significant when considering blooms in other high diatom biomass regions (e.g. Monterey Bay, Santa Barbara Channel; Table 2). And, while the PB09 bloom was much more biologically active by all our proxies, the larger size of the PB08 bloom more than offset the difference in production rates and suggests even diffuse blooms significantly affect regional Si budgets. A caveat to these estimations is that the blooms were clearly sampled in different stages of their development; therefore, the amount of biogenic silica produced in the PB08 bloom is likely underestimated, especially given the higher reported  $\int \rho_P$  by Brzezinski et al. (1998) in this sector of the NPSG during summer (Fig. 6B).

Wilson et al. (2008) demonstrated that blooms in the north-eastern quadrant of the NPSG, near the subtropical front, are significantly larger in area (up to five-fold) and have longer duration than blooms near station ALOHA (i.e. gyre-interior). MODIS [Chl *a*] data between June and October of 2008 and 2009 show strong differences in the extent of blooms in each year of our field study (Fig. 7). A caveat to our analysis is the large amount of cloud cover obscured the study region; therefore, the days a particular location was above our threshold [Chl *a*] (color scale, Fig. 7A and B) are conservative for all areas. By averaging the  $\int \rho_P$  from all three bloom stations during the PB cruises (0.99 mmol Si m<sup>-2</sup> d<sup>-1</sup>), and assuming a 10-day duration (minimum estimate based on MODIS data, Fig. 7A and B) we can extrapolate for the bSiO<sub>2</sub> produced during the 2008 and 2009 bloom seasons in three latitudinal bands (Fig. 7C, Table 2). In both years, the majority of silica production occurred between 30–35°N (Table 2). Overall, in 2008 and 2009 the northern latitude blooms (e.g. 30–35°N) produced 3x and 25x more bSiO<sub>2</sub> than blooms in the gyre interior (e.g. 20–25°N), as a function of the larger bloom area during both years. Given the differences in the size and duration between blooms in the northeastern portion of the gyre and those in the interior near station ALOHA (e.g. Fig. 7), the gyre-interior blooms would have to sustain  $\int \rho_P$  nearly an order of magnitude faster than rates in the north to produce



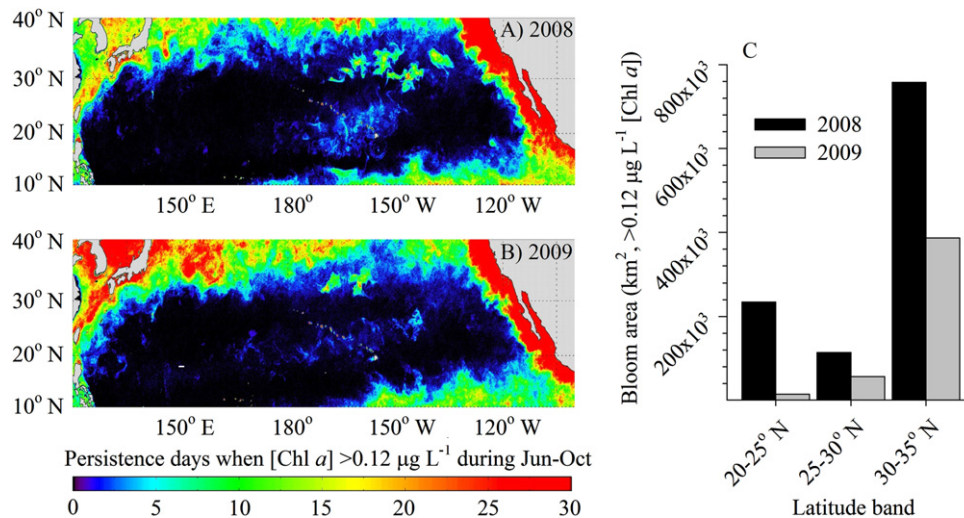


**Fig. 7.** Comparison of 2008 and 2009 bloom seasons in the NPSG using the MODIS dataset. (A and B) days where daily [Chl *a*] was > 0.12 µg L<sup>-1</sup> for 2008 (A) and 2009 (B) between June and October. (C) The area (km<sup>2</sup>) where [Chl *a*] was > 0.12 µg L<sup>-1</sup>; values were binned by latitude and represent the same time period and data from A and B. The longitude considered was between 180–130°W, except for the 30–35°N bin where the only data between 180–135°W was used (to avoid the California Current boundary). Note: Because these use daily MODIS values, the duration of each bloom is potentially underestimated due to cloud cover (i.e. days with no recorded value), this is the case for the PB09 bloom feature which was only successfully viewed during five different days, albeit over a 16-day span.

more bSiO<sub>2</sub> than the northeastern-gyre blooms (Table 2). Considering that the PB08 bloom rate, even under declining conditions, was 49% of the rate observed in the active PB09 bloom, this seems unlikely. While the contribution of diatoms to silica and organic matter production and export is well documented at station ALOHA in the gyre interior (Scharek et al., 1999a, 1999b; Brzezinski et al., 2011; Karl et al., 2012) this analysis suggests that the role of diatom blooms to these processes is even greater in the northeastern reaches of the gyre near the subtropical front.

The temporal resolution of studies reporting Si biogeochemical data in the NSPG outside of station ALOHA is very poor, and not conducive for constructing an annual budget. The northeastern region of the NSPG near the subtropical front zone may operate differently in regards to annual rates of silica production and export than in the gyre interior near station ALOHA as a consequence of spatially larger and longer-persisting blooms (Wilson et al., 2008). Here we demonstrate that there is significant spatial variation in siliceous biomass and production rates in the NSPG during the summer, which may be of biogeochemical importance for a regional Si budget and especially to annual rates diatom silica and carbon export. The northeastern region of the NSPG near the subtropical front, where the most expansive blooms occur, is not amenable to monthly sampling as is done at station ALOHA. However, future studies in this and other sectors of the NSPG could examine processes such export by using passive (e.g. sediment traps) methods or autonomous vehicles (e.g. glider with fluorometer and/or transmissometer) which sample with higher temporal resolution.

## Acknowledgments

We thank J. Jones, E. Allman, C. Beucher, C. Brown, D. Foley, V. Franck, J. Goodman, A. Pyle, K. Rogers, K. Swanson, and S. Vega for logistical and technical assistance, M. Church and S. Duhamel for data access, the Captain, resident technicians and crew of the R/V *Kilo Moana* for assistance at sea. This work was funded by National Science Foundation Ocean Sciences grants OCE-0648130 awarded to MAB, and OCE-0726726 and OCE-0094591 awarded to TAV.

## References

- Arrigo, K.R., van Dijken, G.L., 2004. Annual changes in sea-ice, chlorophyll *a*, and primary production in the Ross Sea, Antarctica. *Deep-Sea Res. II* 51, 117–138.
- Benitez-Nelson, C.R., Bidigare, R.R., Dickey, T.D., Landry, M.R., Leonard, C.L., Brown, S.L., Nencioli, F., Rii, Y.M., Maiti, K., Becker, J.W., Bibby, T.S., Black, W., Cai, W.J., Carlson, C.A., Chen, F.Z., Kuwahara, V.S., Mahaffey, C., McAndrew, P.M., Quay, P.D., Rappe, M.S., Selph, K.E., Simmons, M.P., Yang, E.J., 2007. Mesoscale eddies drive increased silica export in the subtropical Pacific Ocean. *Science* 316 (5827), 1017–1021, <http://dx.doi.org/10.1126/science.1136221>.
- Brzezinski, M.A., 1985. The Si:C:N ratio of marine diatoms: interspecific variability and the effect of some environmental variables. *J. Phycol.* 21 (3), 347–357.
- Brzezinski, M.A., Jones, J.L., Bidle, K.D., Azam, F., 2003. The balance between silica production and silica dissolution in the sea: insights from Monterey Bay, California, applied to the global data set. *Limnol. Oceanogr.* 48 (5), 1846–1854.
- Brzezinski, M.A., Krause, J.W., Church, M.J., Karl, D.M., Li, B., Jones, J.L., Updyke, B., 2011. The annual silica cycle of the North Pacific subtropical gyre. *Deep-Sea Res. I* 58 (10), 988–1001, <http://dx.doi.org/10.1016/j.dsr.2011.08.001>.
- Brzezinski, M.A., Nelson, D.M., 1995. The annual silica cycle in the Sargasso Sea near Bermuda. *Deep-Sea Res. I* 42 (7), 1215–1237.
- Brzezinski, M.A., Phillips, D.R., 1997. Evaluation of Si-32 as a tracer for measuring silica production rates in marine waters. *Limnol. Oceanogr.* 42 (5), 856–865.
- Brzezinski, M.A., Phillips, D.R., Chavez, F.P., Friederich, G.E., Dugdale, R.C., 1997. Silica production in the Monterey, California, Upwelling system. *Limnol. Oceanogr.* 42 (8), 1694–1705.
- Brzezinski, M.A., Villareal, T.A., Lipschultz, F., 1998. Silica production and the contribution of diatoms to new and primary production in the central North Pacific. *Mar. Ecol.-Progress Series* 167, 89–104.
- Calil, P.H.R., Doney, S.C., Yumimoto, K., Eguchi, K., Takemura, T., 2011. Episodic upwelling and dust deposition as bloom triggers in low-nutrient, low-chlorophyll regions. *J. Geophys. Res.-Oceans* 116 (C06030), <http://dx.doi.org/10.1029/2010jc006704>.
- Calil, P.H.R., Richards, K.J., 2010. Transient upwelling hot spots in the oligotrophic North Pacific. *J. Geophys. Res.-Oceans*, 115, <http://dx.doi.org/10.1029/2009jc005360>.
- Church, M.J., Mahaffey, C., Letelier, R.M., Lukas, R., Zehr, J.P., Karl, D.M., 2009. Physical forcing of nitrogen fixation and diazotroph community structure in the North Pacific subtropical gyre. *Global Biogeochem. Cycles*, 23, <http://dx.doi.org/10.1029/2008gb003418>.
- Conley, D.J., Kilham, S.S., Theriot, E., 1989. Differences in silica content between marine and fresh-water diatoms. *Limnol. Oceanogr.* 34 (1), 205–213.
- Demarest, M.S., Brzezinski, M.A., Nelson, D.M., Krause, J.W., Jones, J.L., Beucher, C.P., 2011. Net biogenic silica production and nitrate regeneration determine the strength of the silica pump in the Eastern Equatorial Pacific. *Deep-Sea Res. II* 58 (3–4), 462–476, <http://dx.doi.org/10.1016/j.dsr.2010.08.007>.
- Dore, J.E., Letelier, R.M., Church, M.J., Lukas, R., Karl, D.M., 2008. Summer phytoplankton blooms in the oligotrophic North Pacific subtropical gyre: historical perspective and recent observations. *Prog. Oceanogr.* 76 (1), 2–38, <http://dx.doi.org/10.1016/j.pocan.2007.10.002>.
- Dugdale, R.C., 1967. Nutrient limitation in the sea: dynamics, identification, and significance. *Limnol. Oceanogr.* 12 (4), 685–695.



- Duhamel, S., Bjorkman, K.M., Wambeke, F.V., Moutin, T., Karl, D.M., 2011. Characterization of alkaline phosphatase activity in the North and South Pacific subtropical gyres: implications for phosphorus cycling. *Limnol. Oceanogr.* 56 (4), 1244–1254, <http://dx.doi.org/10.4319/lo.2011.56.4.1244>.
- Duhamel, S., Dyhrman, S.T., Karl, D.M., 2010. Alkaline phosphatase activity and regulation in the North Pacific subtropical gyre. *Limnol. Oceanogr.* 55 (3), 1414–1425, <http://dx.doi.org/10.4319/lo.2010.55.3.1414>.
- Eppley, R.W., Renger, E.H., Venrick, E.L., Mullin, M.M., 1973. A study of plankton dynamics and nutrient cycling in the central gyre of the North Pacific ocean. *Limnol. Oceanogr.* 18 (4), 534–551.
- Fong, A.A., Karl, D.M., Lukas, R., Letelier, R.M., Zehr, J.P., Church, M.J., 2008. Nitrogen fixation in an anticyclonic eddy in the oligotrophic North Pacific Ocean. *ISME J.* 2 (6), 663–676, <http://dx.doi.org/10.1038/ismej.2008.22>.
- Karl, D.M., Christian, J.R., Dore, J.E., Hebel, D.V., Letelier, R.M., Tupas, L.M., Winn, C.D., 1996. Seasonal and interannual variability in primary production and particle flux at Station ALOHA. *Deep-Sea Res.* 43 (2–3), 539–568.
- Karl, D.M., Church, M.J., Dore, J.E., Letelier, R.M., Mahaffey, C., 2012. Predictable and efficient carbon sequestration in the North Pacific Ocean supported by symbiotic nitrogen fixation. *PNAS* 109 (6), 1842–1849, <http://dx.doi.org/10.1073/pnas.1120312109>.
- Krause, J.W., Brzezinski, M.A., Jones, J.L., 2011. Application of low level beta counting of <sup>32</sup>Si for the measurement of silica production rates in aquatic environments. *Mar. Chem.* 127, 40–47, <http://dx.doi.org/10.1016/j.marchem.2011.07.001>.
- Krause, J.W., Brzezinski, M.A., Landry, M.R., Baines, S.B., Nelson, D.M., Selph, K.E., Taylor, A.G., Twining, B.S., 2010a. The effects of biogenic silica detritus, zooplankton grazing, and diatom size structure on silicon cycling in the euphotic zone of the eastern equatorial Pacific. *Limnol. Oceanogr.* 55 (6), 2608–2622, <http://dx.doi.org/10.4319/lo.2010.55.6.2608>.
- Krause, J.W., Brzezinski, M.A., Villareal, T.A., Wilson, C., 2012. Increased kinetic efficiency for silicic acid uptake as a driver of summer diatom blooms in the North Pacific subtropical gyre. *Limnol. Oceanogr.* 57, 4.
- Krause, J.W., Nelson, D.M., Lomas, M.W., 2009. Biogeochemical responses to late-winter storms in the Sargasso Sea, II: increased rates of biogenic silica production and export. *Deep-Sea Res.* 56 (6), 861–874, <http://dx.doi.org/10.1016/j.dsr.2009.01.002>.
- Krause, J.W., Nelson, D.M., Lomas, M.W., 2010b. Production, dissolution, accumulation and potential export of biogenic silica in a Sargasso Sea mode-water eddy. *Limnol. Oceanogr.* 55 (2), 569–579.
- McGillicuddy, D.J., Anderson, L.A., Bates, N.R., Bibby, T., Buesseler, K.O., Carlson, C.A., Davis, C.S., Ewart, C., Falkowski, P.G., Goldthwait, S.A., Hansell, D.A., Jenkins, W.J., Johnson, R., Kosnyrev, V.K., Ledwell, J.R., Li, Q.P., Siegel, D.A., Steinberg, D.K., 2007. Eddy/Wind interactions stimulate extraordinary mid-ocean plankton blooms. *Science* 316 (5827), 1021–1026.
- McGillicuddy, D.J., Robinson, A.R., Siegel, D.A., Jannasch, H.W., Johnson, R., Dickey, T., McNeil, J., Michaels, A.F., Knap, A.H., 1998. Influence of mesoscale eddies on new production in the Sargasso Sea. *Nature* 394 (6690), 263–266.
- Nelson, D.M., Ahern, J.A., Herlihy, L.J., 1991. Cycling of biogenic silica within the upper water column of the Ross Sea. *Mar. Chem.* 35, 461–476.
- Ragueneau, O., Treguer, P., 1994. Determination of biogenic silica in coastal waters—applicability and limits of the alkaline digestion method. *Mar. Chem.* 45 (1–2), 43–51, [http://dx.doi.org/10.1016/0304-4203\(94\)90090-6](http://dx.doi.org/10.1016/0304-4203(94)90090-6).
- Scharek, R., Latasa, M., Karl, D.M., Bidigare, R.R., 1999a. Temporal variations in diatom abundance and downward vertical flux in the oligotrophic North Pacific gyre. *Deep-Sea Res.* 46 (6), 1051–1075.
- Scharek, R., Tupas, L.M., Karl, D.M., 1999b. Diatom fluxes to the deep sea in the oligotrophic North Pacific gyre at Station ALOHA. *Mar. Ecol. Progress Series* 182, 55–67.
- Shcherbina, A.Y., Gregg, M.C., Alford, M.H., Harcourt, R.R., 2009. Characterizing thermohaline intrusions in the North Pacific subtropical frontal zone. *J. Phys. Oceanogr.* 39 (11), 2735–2756, <http://dx.doi.org/10.1175/2009jpo4190.1>.
- Shcherbina, A.Y., Gregg, M.C., Alford, M.H., Harcourt, R.R., 2010. Three-dimensional structure and temporal evolution of submesoscale thermohaline intrusions in the North Pacific subtropical frontal zone. *J. Phys. Oceanogr.* 40 (8), 1669–1689, <http://dx.doi.org/10.1175/2010jpo4373.1>.
- Shipe, R.F., Brzezinski, M.A., 2001. A time series study of silica production and flux in an eastern boundary region: Santa Barbara Basin, California. *Global Biogeochem. Cycles* 15 (2), 517–531.
- Shipe, R.F., Brzezinski, M.A., Pilska, C., Villareal, T.A., 1999. Rhizosolenia mats: an overlooked source of silica production in the open sea. *Limnol. Oceanogr.* 44 (5), 1282–1292.
- Sverdrup, H.U., 1953. On conditions for the vernal blooming of phytoplankton. *ICES J. Mar. Sci.* 18 (3), 287–295.
- Venrick, E.L., 1988. The vertical distributions of chlorophyll and phytoplankton species in the North Pacific central environment. *J. Plankton Res.* 55, 987–998.
- Venrick, E.L., 1997. Comparison of the phytoplankton species composition and structure in the climax area (1973–1985) with that of station ALOHA (1994). *Limnol. Oceanogr.* 42 (7), 1643–1648.
- Villareal, T.A., Adornato, L., Wilson, C., Schoenbaechler, C.A., 2011. Summer blooms of diatom–diazotroph assemblages and surface chlorophyll in the North Pacific gyre: a disconnect. *J. Geophys. Res.-Oceans* 116 (C03001), 15, <http://dx.doi.org/10.1029/2010jc006268>.
- Villareal, T.A., Brown, C.G., Brzezinski, M.A., Krause, J.W., Wilson, C., 2012. Summer diatom blooms in the North Pacific subtropical gyre: 2008–2009. *PLoS One* 7 (4), e33109, <http://dx.doi.org/10.1371/journal.pone.0033109>.
- Watkins-Brandt, K.S., Letelier, R.M., Spitz, Y.H., Church, M.J., Boettjer, D., White, A.E., 2011. Addition of inorganic or organic phosphorus enhances nitrogen and carbon fixation in the oligotrophic North Pacific. *Mar. Ecol. Progress Series* 432, 17–29, <http://dx.doi.org/10.3354/meps09147>.
- Welschmeyer, N.A., 1994. Fluorometric analysis of chlorophyll a in the presence of chlorophyll b and pheopigments. *Limnol. Oceanogr.* 39 (8), 1985–1992.
- Wilson, C., 2003. Late summer chlorophyll blooms in the oligotrophic North Pacific subtropical gyre. *Geophys. Res. Lett.* 30 (18), <http://dx.doi.org/10.1029/2003gl017770>.
- Wilson, C., 2011. Chlorophyll anomalies along the critical latitude at 30 degrees N in the NE Pacific. *Geophys. Res. Lett.* 38, <http://dx.doi.org/10.1029/2011gl048210>.
- Wilson, C., Villareal, T.A., Brzezinski, M.A., Krause, J.W., Shcherbina, A.Y., in review. Chlorophyll Bloom Development and the Subtropical Front in the North Pacific.
- Wilson, C., Villareal, T.A., Maximenko, N., Bograd, S.J., Montoya, J.P., Schoenbaechler, C.A., 2008. Biological and physical forcings of late summer chlorophyll blooms at 30 degrees N in the oligotrophic Pacific. *J. Mar. Sys.* 69 (3–4), 164–176, <http://dx.doi.org/10.1016/j.jmarsys.2005.09.018>.